JOURNAL OF SOLID STATE CHEMISTRY 118, 84–92 (1995)

Kinetics and Mechanism of Molybdenum (VI) Oxide Reduction

Jerzy Słoczyński

Institute of Catalysis and Surface Chemistry, Polish Academy of Sciences, ul. Niezapominajiek, 30-239 Kraków, Poland

Received August 11, 1994; in revised form January 11, 1995; accepted January 17, 1995

Kinetics of the reduction of MoO_3 under hydrogen, propene, butene-1, and CO has been studied. It has been found that MoO_3 morphology and the addition of MoO_2 and metallic platinum affect the rate of reduction under hydrogen. The experimental findings confirm the validity of the CAR model proposed earlier, according to which the reduction of MoO_3 to MoO_2 is a consecutive reaction and Mo_4O_{11} is the intermediate product. The dissociative adsorption of the reductant yielding atomic hydrogen is the rate-determining step. The process is autocatalytically accelerated by the reaction product, MoO_2. © 1995 Academic Press, Inc.

INTRODUCTION

Reduction of MoO_3 by hydrogen is one of the methods used to obtain metallic molybdenum of high purity. The reduction to lower oxides is of interest because molybdenum (VI) oxide is a main component of catalysts for selective oxidation of olefins (1), ammoxidation of toluene (2, 3), and hydrodesulfurization of oil (4).

The kinetics of the reduction of MoO_3 to MoO_2 was investigated by many authors (5–18). In a number of papers (6–8, 10, 11, 13, 15) on the reduction of MoO_3 by hydrogen or hydrocarbons, a sigmoidal shape of the $\alpha(t)$ (degree of reduction versus time) curves has been observed, which indicates that the rate of reaction goes through a maximum. In only a few papers, has the linear dependence of α versus time been reported (5, 9, 12).

The sigmoidal shape of the $\alpha(t)$ curves is often described by the Avrami–Erofeev equation (19), which assumes that nucleation of the solid product of reduction is the rate-determining step. An alternative explanation for the increase in the rate of reduction has been proposed by Słoczyński (16). The author has postulated that the dissociative adsorption of hydrogen is the rate-determining step and that the acceleration of the reaction is due to an autocatalytic effect.

Phase composition in the MoO_3–MoO_2 range has been intensely investigated with the use of mainly XRD (11, 15, 20–27). The existence of seven intermediate oxides of defined structure was established. Early stages of the MoO_3 reduction, prior to the formation of the reduction products in the form of separate phases, have been described by Bursil (28), Thöni and Hirsch (29, 30), and Gai (31, 32). In the discussed case, oxygen vacancies originating in the course of the reduction disappear as the result of the formation of shear planes without any change in the structure of the parent oxide. Changes in the surface composition of MoO_3 during reduction have been investigated with the use of ESCA (33–35), whereas an ESR technique has been used to determine the oxidation state of molybdenum and its coordination (36–38). Molybdenum bronzes of the composition H_xMoO_3 are formed in the course of a low-temperature reduction of MoO_3 (39–42). In this case, the reduction proceeds with the participation of atomic hydrogen, which is formed in the presence of small amounts of metallic platinum or palladium and migrates to the oxide phase (a spillover effect). Acceleration of the reduction of MoO_3 due to a slight admixture of Pt or Pd was observed by many authors (43–47). The effect of a support on the rate of MoO_3 reduction was also reported (18, 48), but the problem has not been investigated systematically.

In many papers, the reduction of molybdenum (VI) oxide to MoO_2 has been considered a one-step reaction. Burch (11) was the first to suggest that Mo_4O_{11} was an intermediate product of the reduction. This hypothesis was confirmed experimentally by Ueno *et al.* (15), who investigated the reduction of MoO_3 by an X-ray high-temperature technique.

In a subsequent paper by Słoczyński and Bobiński (17), a detailed kinetic analysis of the consecutive autocatalytic reaction (CAR) model has been carried out. The authors have shown that the CAR model describes kinetics of the reduction of molybdenum (VI) oxide, unsupported and deposited on different supports (18).

In the present work, a number of experiments confirming the autocatalytic character of the MoO_3 reduction and elucidating the reaction mechanism have been presented.

EXPERIMENTAL

Three preparations of molybdenum oxide were investigated: I, obtained by thermal decomposition of ammo-

0022-4596/95 $12.00

nium paramolybdate at 623 K followed by heating the solid residue at 823 K for 5 hr; II, a commercial reagent from POCH; and III, obtained by a sublimation of I at 1100 K. MoO_2 was obtained by reduction of I under hydrogen at 823 K and cooling under vacuum to room temperature.

The preparations were characterized by: (i) determination of specific surface area with the BET method using krypton as an adsorbate; (ii) an X-ray diffraction method using a DRON-2 diffractometer and Cu$K\alpha$ radiation; and (iii) observations in a Nikon optical polarization microscope in reflected light.

Contents of the crystalline components of the reaction mixtures were determined from the relative intensities of selected X-ray diffraction maxima: at 3.27 Å for MoO_3, at 4.00 Å for Mo_4O_{11}, and 3.41 Å for MoO_2. Three component mixtures of known composition were used as standards for the calibration. Details of the procedure employed are given in (18).

The rate of reduction was measured with a Sartorius vacuum microbalance connected to a standard vacuum system. Details of the measurements were given in the earlier work (18). The pulse experiments were carried out in a flow microreactor coupled to a gas chromatograph with a thermal conductivity detector, using helium as a carrier gas.

Several reducing gases were employed: (i) commercial hydrogen which was purified by passing through a palladium filter at 623 K; (ii) carbon monoxide from Merck (≥99% CO); and (iii) propene and butene-1 from Phillips Petroleum (pure grade).

RESULTS

Characteristics of the Preparations

Chemical and spectral analyses have shown that the content of metallic impurities in the MoO_3 preparations investigated does not exceed 0.01%. The content of nitrogen present as ammonium ion is on the order of 0.01%, and that of nitrogen in the form of NO_3 is below this value. The surface area is 1, 0.1, and 0.015 m^2/g for preparations I, II, and III respectively.

Molybdenum (VI) oxide has a tendency to form single crystals in the shape of thin plates. Their large faces (basal) coincide with the (0k0) lattice planes whereas side faces are (100) and (001) (e.g., 51, 56, 58).

Microscopic observations have revealed that the preparation obtained through sublimation (III) consists of well-developed plate-shaped crystals of average dimensions (4–10 mm) × (0.2–2 mm) × (0.01–0.2 mm). The commercial preparation (II) consists of small well-formed crystals in the shape of thin platelets or plates. It is similar to sublimated MoO_3 but is microcrystalline. In contrast, molybdenum oxide obtained by the decomposition of ammonium paramolybdate (I) forms skeleton polycrystalline

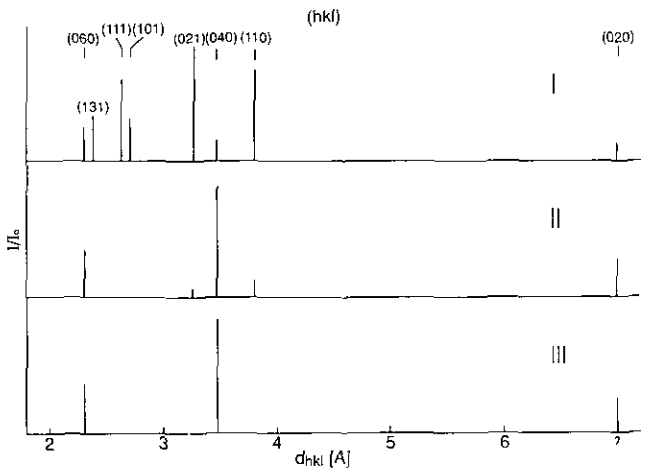

FIG. 1. X-ray patterns for MoO_3 preparations of various morphologies.

aggregates built of microcrystals of dimensions 3–9 μm, similar in all directions. It should be thus surmised that the fraction of basal faces (0k0) and side faces (100) and (001) will be similar in preparation I whereas the basal faces will prevail in preparations II and III.

Result of the X-ray investigations shown in Fig. 1 confirm this supposition. Since crystallites in preparation I fulfill the condition of random orientation in an X-ray diffraction experiment, intensities of the reflections coming from different lattice planes agree with the standard values listed in ASTM. In contrast, the preparations of the plate morphology (II and III) show a tendency to have an orientation parallel to the basal faces, hence the reflections (0k0) are markedly stronger compared to the ASTM values.

Phase Transformations during Reductions

The X-ray diffraction has shown that the reduction of the investigated preparations of MoO_3 at temperatures below 823 K is a two-step process whereby Mo_4O_{11} is an intermediate and MoO_2 is a final product of the reduction, irrespective of the reductant used. No other suboxides of molybdenum have been found. This observation agrees with our earlier findings (18) as well as with the results of other authors (2, 9, 11, 14). The reduction reaction may be thus written as

$$\underset{(A)}{MoO_3} \rightarrow \underset{(B)}{Mo_4O_{11}} \rightarrow \underset{(C)}{MoO_2}. \qquad [1]$$

Contents of the above compounds as a function of the degree of reduction (α) are compared for the reductants hydrogen and butene in Fig. 2. As one can see, the A → B reaction is faster than B → C for the reduction under hydrogen. As a result, the content of the intermediate

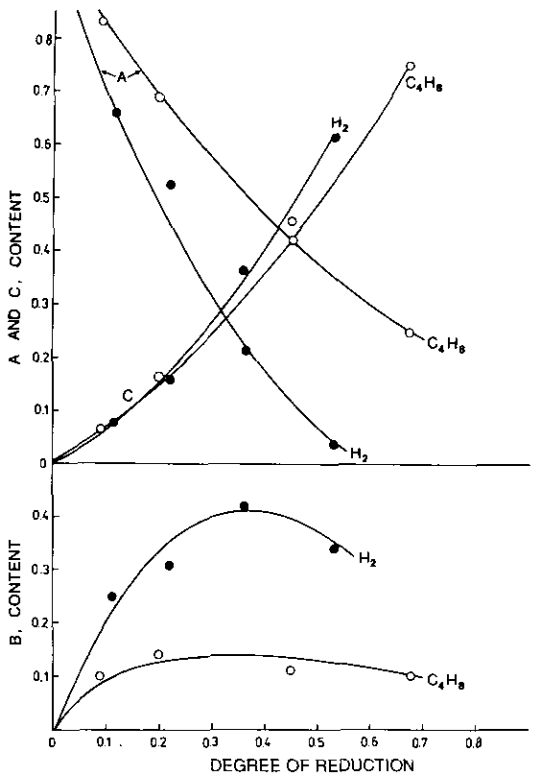

FIG. 2. Changes in phase compositions during reduction of MoO_3 under hydrogen and under butene-1. H_2: T = 823 K, p = 26.6 Kpa; butene-1: T = 793 K, p = 7.0 kPa.

reduction product close to a maximum is comparatively high, whereas it is low for butene and it changes little in the course of the reduction. This indicates that in the case of the reduction by butene, rates of the two reactions A → B and B → C are comparable. The phase composition of samples reduced by propene is similar to that found for the samples reduced under butene.

Microscopic observations of the reduced samples have shown that products of the MoO_3 reduction crystallize in loose aggregates and do not form a compact layer at the oxide surface, which would hamper access of the reductant. A "fresh" surface of the MoO_3 grains is permanently accessible and it diminishes with the progress of the reaction, according to the "shrinking core" model (49).

Investigations carried out with the pulse technique have shown that products of coking are deposited on surfaces of samples reduced by hydrocarbons. The experiments consisted in the reduction of MoO_3 in a flow reactor by pulses of propene or butene, followed by the reoxidation by pulses of oxygen. The degree of coking of the reduced samples could be established from the amount of CO_2 formed in the course of combusting the carbon deposit. It has been found that the amount of the carbon deposit increases in proportion to the degree of reduction of MoO_3. Formation of the products of coking in the course of the reduction of MoO_3 by butene was also observed by Batist *et al.* (6).

Reduction Kinetics

Figure 3 shows the initial rate of MoO_3 reduction as a function of pressure, for different reductants. As one can see the rate of reduction is proportional to the pressure, hence the reaction is of the first order with respect to gaseous reductant.

Figure 4 shows full kinetic curves for the reduction by hydrogen in the form of plots of the rate of reduction as a function of the degree of reduction, for three MoO_3 preparations described above, differing in the crystallite morphology. Due to considerable differences in the reaction rates resulting from different surface areas of the preparations, ratios of the current rate of reduction R to the initial rate of reduction R_0 were plotted. Values of the rates of reduction in Fig. 4 have been recalculated for the same hydrogen pressure of 1 Pa. Hence, the differences which one can see in the figure reflect differences in the morphologies of preparations I–III.

The effect of the nature of reductant used was investigated for preparation I. Figure 5 shows the rate of reduction R as a function of the degree of reduction (α) for propene and butene-1 at various temperatures. The analogous set of curves for the reduction by hydrogen is given in Ref. (18). For both propene and butene-1 the position of the maximum shifts with an increase in the temperature toward smaller values of α and at the same time its height

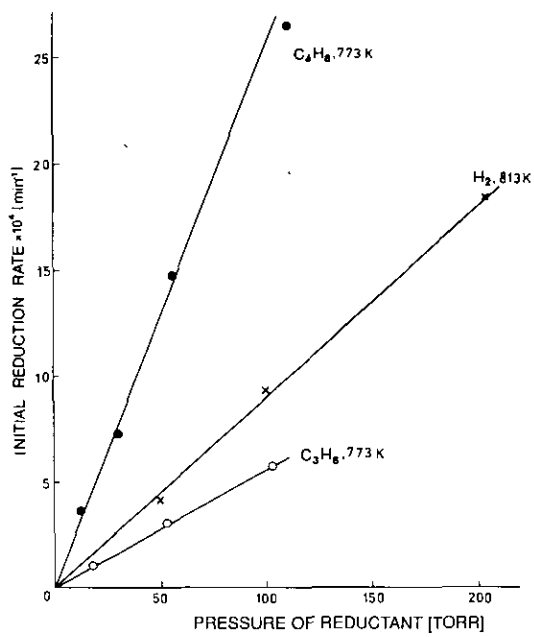

FIG. 3. Initial rate of reduction of MoO_3 (preparation I) as a function of pressure for various reductants.

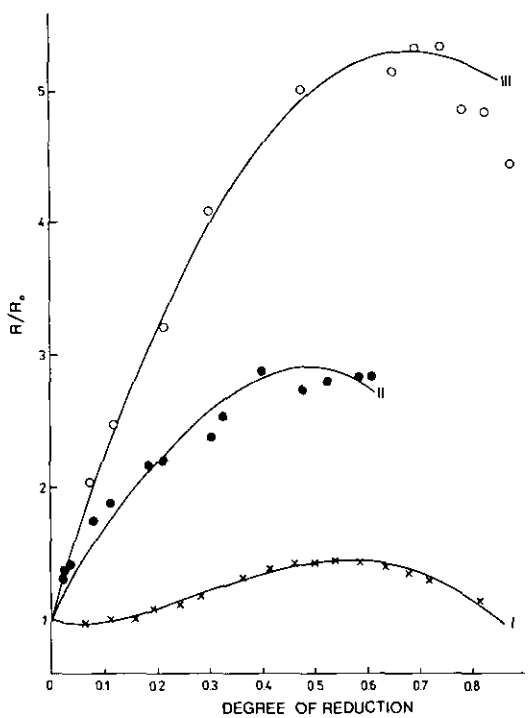

FIG. 4. Kinetics of reduction by hydrogen of preparations of MoO_3 differing in morphology, $T = 813$ K. (I) $R_0 = 9.75 \times 10^{-11}$ $s^{-1}Pa^{-1}$, $k = 1.0$, $\kappa = 0.10$; (II) $R_0 = 3.08 \times 10^{-10}$ $s^{-1}Pa^{-1}$, $k = 2.9$, $\kappa = 0.16$; (III) $R_0 = 1.13 \times 10^{-9}$ $s^{-1}Pa^{-1}$, $k = 5.1$, $\kappa = 0.11$.

increases. In the case of hydrogen, the position of the maximum on the $R(\alpha)$ curve does not depend on the temperature and corresponds to $\alpha \approx 0.5$.

The initial rates of reduction are compared for various reductants in Fig. 6 in the form of linear Arrhenius plots in the coordinate system ln R_0 versus $1/T$. As one can see, the rate of reduction increases in the order: CO < H_2 < C_3H_6 < C_4H_8. The differences are very large and amount to several orders of magnitude. The activation energy of the reduction decreases in the same order. It is 125 ± 5 kJ $mole^{-1}$ for H_2, 113 ± 10 kJ $mole^{-1}$ for propene, and 80 ± 10 kJ $mole^{-1}$ for butene-1 and correlates with values of energy required to abstract one atom of hydrogen from the gaseous reductant; these values, expressed in kJ $mole^{-1}$, are: 432.7 (H_2), 361.2 (propene), and 328.1 (butene-1) (50). For comparison, the activation energy of the reduction in CO is 137 ± 10 kJ $mole^{-1}$, i.e., is higher than that of any hydrogen-containing reductant.

In order to confirm the autocatalytic course of the reduction, experiments with an admixture of MoO_2 have been performed. Preparation I has been used with hydrogen as the reductant. The results are shown in Fig. 7 in the form of the $R(\alpha)$ curves. As one can see, the addition of the final product of the reduction, i.e., MoO_2, clearly increases the initial rate of MoO_3 reduction. The maximum on the $R(\alpha)$ curve shifts slightly toward smaller values of α, at the same time a decrease in its relative height, the measure of which is the R_m/R_0 ratio, is observed (R_m is a maximum rate of reduction).

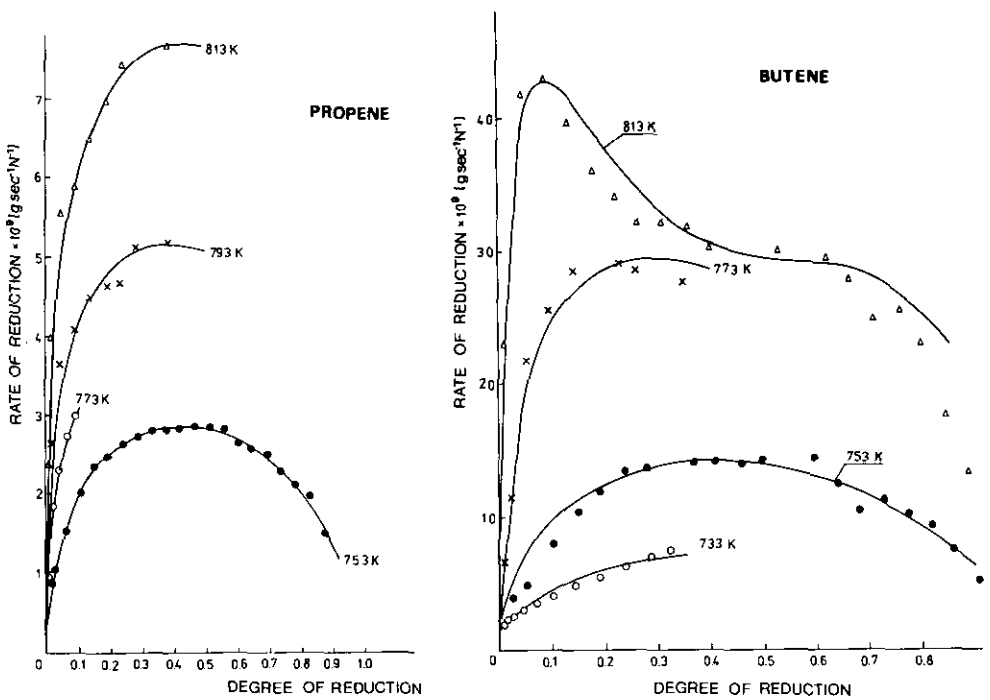

FIG. 5. Kinetics of reduction of MoO_3 (preparation I) by propene and butene-1 at various temperatures. The rate of reduction is recalculated for a reductant pressure of 1 Pa and a specific surface area of MoO_3 of 1 m^2g^{-1}.

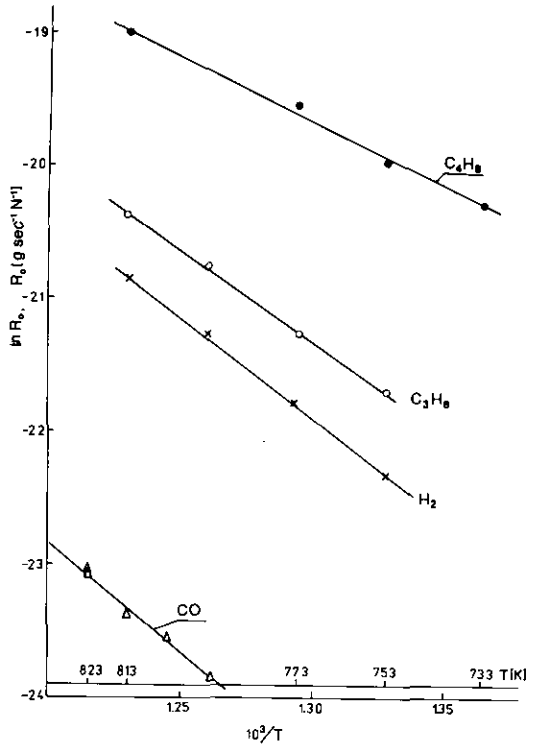

FIG. 6. Arrhenius plots for the initial rate of reduction for MoO_3 (preparation I).

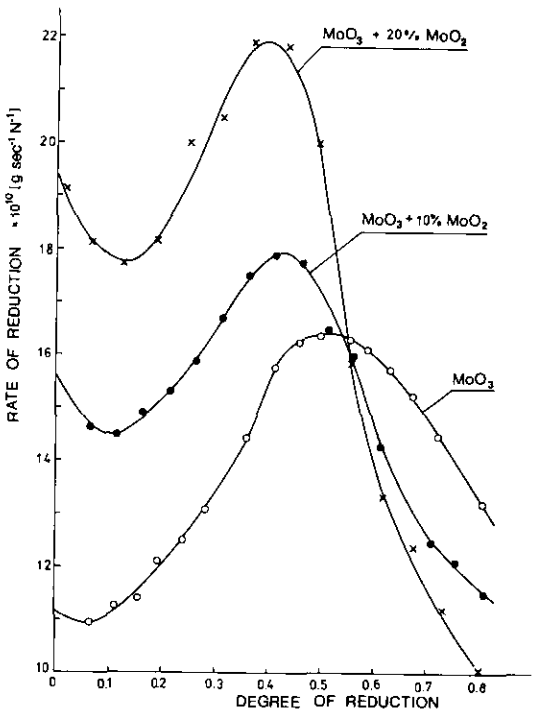

FIG. 7. Effect of addition of MoO_2 on the rate of reduction of MoO_3 (preparation I) at 813 K.

The effect of the addition of platinum on the rate of reduction of MoO_3 was also investigated. Platinum is a known activator of the dissociative adsorption of hydrogen. Platinum black obtained by thermal decomposition of the chloroplatinic acid was used for this purpose. The results are shown in Fig. 8. As one can see, adding Pt increases the initial rate of reduction of MoO_3 10–50 times. The rate decreases with time due to the deactivation of Pt.

DISCUSSION

Analysis of the $R(\alpha)$ kinetic curves for the reduction under hydrogen was carried out on the basis of a consecutive autocatalytic reaction model (CAR), described in detail previously (17).

The autocatalytic action of product C consists in facilitating a dissociative adsorption of the reductant which leads to the formation of reactive atomic hydrogen and transport of the active species to the surface of substrate A (spillover effect). The traces of dispersed metal usually present in the lower oxide which is the final product of the reduction may activate the hydrogen or hydrocarbons used as the reductants.

An obvious condition for the occurrence of the catalytic effect is the existence of contacts between grains of catalyst C and the oxide under reduction. Thus the autocatalytic effect should be particularly pronounced in the reduction of the intermediate product B transforming directly into the final product C, which facilitates the generation of a significant number of the contacts B/C. In contrast, crystallites C do not often contact the substrate A and hence the active hydrogen transfer from C to A is negligible. The above considerations lead to the conclusion that only the second step of the reduction is autocatalytic.

The overall rate of reduction may be expressed in the form of a product $r(p, T) \cdot S(\alpha)$, where the first component accounts for the dependence of the rate on the temperature and pressure of the reductant, and the second reflects the change in size of the reaction interface during the process. If nucleation and crystallization of the products are fast, as indicated by the microscopic observations, $S(\alpha)$ decreases with increasing α, according to the shrinking core model mentioned earlier. Then at constant p, T the rate of consumption of substrate A or intermediate product B is proportional to the surface of unreacted grains, i.e., to the nth power of the actual reactant content. The exponent n is 2/3 for spherical grains and is close to zero for flat platelets of small thickness. Thus, the following scheme corresponds to the CAR model:

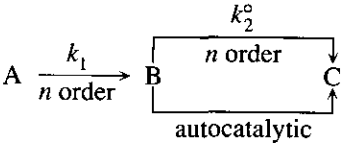

[2]

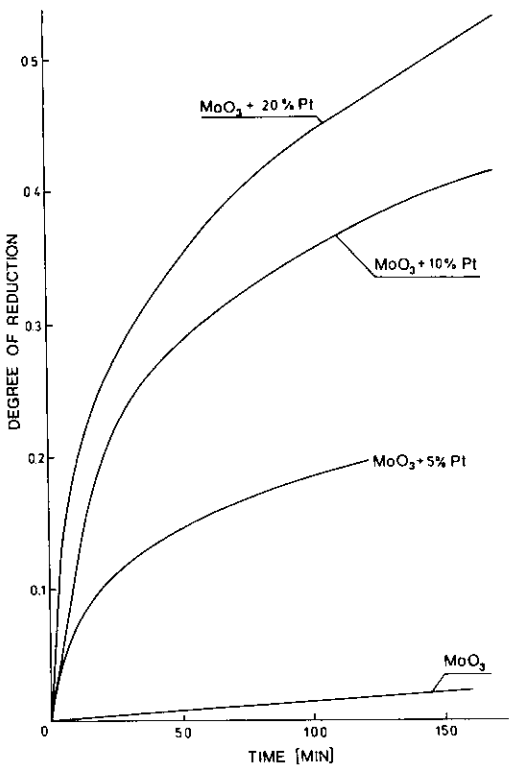

FIG. 8. Effect of addition of Pt on the rate of reduction of MoO_3 (preparation I) at 813 K.

The rates of the subsequent steps of the reduction are described by the set of differential equations

$$-\frac{dx_A}{dt} = k_1 x_A^n; \quad \frac{dx_B}{dt} = \frac{dx_A}{dt} - \frac{dx_C}{dt}; \qquad [3]$$
$$\frac{dx_C}{dt} = k_2 x_B^n \ (\kappa + x_C^n),$$

where x_A, x_B, and x_C are mole fractional contents of the solid reactants. The constant $\kappa = k_2^\circ/k_2$ formally gives the ratio of the rate constants of the noncatalyzed and autocatalyzed reactions. It may also describe the initial amount of the catalyst introduced into the system or formed *in situ* as a result of the appropriate treatment of the sample prior to the reduction.

The rate of reduction determined experimentally may be related to changes in the phase composition by the equation

$$R = R_0[x_A^n + (\delta - 1)kx_B^n(\kappa + x_C^n], \qquad [4]$$

where $R_0 = k_1/\delta$ is the initial rate of reduction, $k = k_2/k_1$, and δ is a constant dependent on the reduction stoichiometry; $\delta = 4$ for reaction [1]. The mole fraction x_A appearing in Eq. [4] may be calculated after integration of the first relationships in Eq. [3], whereas x_B and x_C may be calculated from the experimentally determined degree of reduction α making use of the relations

$$\frac{1}{\delta}x_B + x_C = \alpha, \quad x_A + x_B + x_C = 1. \qquad [5]$$

Rate constants k and κ, and hence k_2 and k_2°, can be calculated by fitting the experimental data into Eq. [4].

Equation [4] has been used to describe the kinetic curves $R(\alpha)$ obtained for the reduction of various preparations of MoO_3 by hydrogen. The number n was assumed to be $\frac{2}{3}$ for preparations I and II and for all the reactants (A, B, C), whereas for the plate-shaped preparation III, which consists of large well-developed crystals, $n = 0$ was assumed for substrate A (MoO_3) and $n = \frac{2}{3}$ for the remaining reactants. The solid lines in Fig. 4 were plotted according to the above assumptions and Eq. [4]. The respective values of constants k and κ, as well as the initial rates of reduction R_0, are given in the caption of the figure.

The data show that the kinetics of reduction depends on the morphology of MoO_3. One can easily determine that the initial rate of reduction (given in the caption of the figure) does not change in proportion to the relative surface area, as was observed previously for preparation I (18). This indicates that the preparations studied have different relative activities which increase with an increase in the fraction of the basal faces ($0k0$). The acceleration of the first step of the reduction (A $\rightarrow$ B), without a significant change in the rate of the second step, leads to an increase in the height of maxima in curves $R(\alpha)$, observed for preparations II and III.

One cannot, however, formulate unequivocal conclusions about the activity of a specific lattice plane of MoO_3 on this basis. Results of investigations on the role of specific faces of MoO_3 crystallites in the catalytic reactions of oxidation of olefins (51–55), alcohols (56, 57), as well as oxidative ammonolysis of toluene (3), obtained by various authors reveal a number of discrepancies which could not be rationally accounted for in the past. Recently it turned out, however, that the basal planes in MoO_3 are not smooth in atomic scale, but have a stepped structure (58). They also thus contain arrangements of atoms characteristic of side planes (e.g., (100)), as well as atoms situated on edges of the steps, having different coordination and energetic properties.

Similar results have been obtained by Mingot *et al.* (59) and Abon *et al.* (60), which prepared MoO_3 by oxidation of the molybdenum foil. Preparations thus obtained have a distinct [100] preferred orientation and are bordered by (110), (120), and (130) faces, which are stepped surfaces composed of (100) terraces and normal (010) steps.

The kinetics of MoO_3 reduction in the atmosphere of

hydrocarbons may be analyzed using the same model but with modifications that take into account the different phase composition of reduced samples. As described earlier, in the case of hydrocarbons, the content of the intermediate product B is small and practically constant in the course of the whole reduction process. Hence, A/C intergranular contacts prevail in the reduced samples, and the number of B/C contacts is limited. This allows one to define reaction [1] as a simple autocatalytic reaction A → C and to neglect the intermediate product B. In these conditions the rate of reduction may be described by the equation

$$-\frac{dx_A}{dt} = k_1^\circ x_A^{2/3} + k_1 x_A^{2/3} x_C^{2/3}, \qquad [6]$$

which, when it is assumed that x_A is proportional to $1 - \alpha$ and x_C to α, may be written as

$$R = \frac{d\alpha}{dt} = R_0(1 + k\alpha^{2/3})(1 - \alpha)^{2/3}, \qquad [7]$$

where $k = k_1^\circ/k_1$.

An additional factor which should be taken into account for the reduction by hydrocarbons is the deposition of products of coking on the surface. Based on the results of the pulse experiments, it has been established that the rate of reduction of MoO_3 by hydrocarbons may be described by the equation

$$R = (R_0 + k_r\alpha^{2/3} - k_C\alpha)(1 - \alpha)^{2/3}, \qquad [8]$$

where the expression $k_C\alpha$ is the rate of accumulation of the carbon deposit on the sample surface, and k_C is the coking constant. Plots in Fig. 5 show the fit to Eq. [8]. Only in the case of reduction by butene at 813 K, where the rate of coking is very high, was the $k_C\alpha/(1 + \alpha)$ expression used instead of $k_C\alpha$, since the former takes into account the hampering of the coke deposition process with increasing degree of reduction. The activation energy of coking is high and amounts to 200 kJ mole^{-1} and 340 kJ mole^{-1} for propene and butene-1, respectively. Hence, the contribution from the coking process increases dramatically with increasing temperature. The coking is negligible below 750 K.

A summary of the most important experimental findings seems necessary before discussing the mechanism of the reduction of MoO_3:

(i) The rate of reduction is proportional to the pressure of the reductant,

(ii) The rate of reduction depends on the nature of the reductant; for hydrogen and alkenes, the rate of reduction increases with decreasing energy necessary to abstract an atom of hydrogen from a molecule of the reductant. The activation energy of reduction decreases in the same order.

(iii) The rate of reduction changes in a complex way with increasing degree of reduction; it passes through a minimum and a maximum or it attains a maximum only. When alkenes are used as reductants, the reduction is accompanied by the formation of the coke deposit, which leads to a decrease in the rate of reduction.

(iv) In the temperature range 723–823 K, the reduction of MoO_3 is a consecutive reaction, orthorombic Mo_4O_{11} is an intermediate product, and MoO_2 is the final product.

(v) Adding MoO_2, the final product of the reduction, accelerates both transitions: $MoO_3 \rightarrow Mo_4O_{11}$ and $Mo_4O_{11} \rightarrow MoO_2$.

(vi) Adding platinum black, a known activator of the dissociative adsorption of H_2, markedly accelerates the reduction of MoO_3.

All the above relationships indicate that the reduction of MoO_3 proceeds according to a previously described model of an autocatalytic consecutive reaction corresponding to kinetic scheme [2]. According to the CAR model, the rate-determining step of the process is the dissociative adsorption of the reductant accelerated autocatalytically by the product of the reduction, MoO_2. The remaining elementary processes, such as the reaction of the surface atomic hydrogen with lattice oxygen, the crystallization of the solid products of the reduction, and the transport of reactants, are fast. The surface area of reduced grains is not blocked by the products of the reduction and it diminishes in the course of the reduction according to the shrinking core model.

Alternative models of the MoO_3 reduction, described in some papers, which assume nucleation to be a rate-determining step, cannot account for all experimental findings. In particular, they exclude the presence of a minimum and a maximum on the curve $R(\alpha)$, whereas such shapes are in fact observed under appropriate conditions. If one assumed that nucleation was the rate-determining step, it would be difficult to explain the accelerating action of platinum or the increase in the rate of reaction $MoO_3 \rightarrow Mo_4O_{11}$ when MoO_2 is added. Nor can the observed correlation between the activation energy and the rate of reduction of MoO_3 on one side, and the energy required for abstraction of hydrogen from a molecule of the reductant on the other, find explanation on the ground of the nucleation model; it is, however, a simple consequence of the CAR model.

Yet other rate-determining steps in the reduction of MoO_3 were considered in older literature. Since in the course of the reaction oxygen vacancies are formed in the subsurface layer, a diffusion stream of oxygen ions from the bulk of crystallites to the surface is generated.

As a result, the concentration of vacancies in the bulk constantly increases, which leads, when a certain limit is exceeded, to the formation of new phases of lower oxides. Using such reasoning, Batist *et al.* (6) developed a model of the MoO_3 reduction, which assumes the diffusion of O^{2-} ions from the bulk to the surface to be the rate-determining step and the activation energy to be equal to the activation energy of the diffusion step. The model was next improved by Steenhof de Jong *et al.* (61), without principally altering, however, its physical basis.

In the light of the facts observed, the models based on the assumption that the diffusion of the lattice oxygen is a step limiting the reduction of MoO_3 are inadequate. They do not account for the shapes of the kinetic curves nor for the acceleration of the reaction on the addition of MoO_2. Obviously one should expect that the addition of platinum or a change in the kind of reductant would lead to an increase in the hydrogen concentration, which would accelerate the surface reaction. A faster depletion of oxygen from the surface layer would increase the concentration gradient, and hence the diffusion stream of oxygen ions. However, all these processes cannot change the activation energy of the oxygen diffusion. Thus the observed decrease in the activation energy of reduction which accompanies the change in the reductant from hydrogen to alkenes cannot be explained within the framework of the diffusion model.

The diffusion model can also be criticized on broader grounds. It is known from the investigations cited in the Introduction that atomic hydrogen readily penetrates the bulk of MoO_3 already at room temperature. One should thus expect that at elevated temperatures the reduction of the subsurface layer will proceed even more as the result of the migration of atomic hydrogen into the oxide structure. Under such conditions the diffusion of the lattice oxygen is not necessary, since the oxygen deficit is quickly compensated for by the crystallization of the reduction products (oxides impoverished in oxygen) and the uncovering of fresh surfaces of unreacted MoO_3. Diffusion of the oxygen lattice and formation of the oxygen vacancies play a significant role in the formation of shear planes in the earlier stages of the reduction before new oxide phases appear. These processes may be observed during the reduction of MoO_3 at low temperature.

ACKNOWLEDGMENT

The assistance of Ms. Z. Czuła in carrying out lengthy measurements of the rate of reduction is gratefully acknowledged.

REFERENCES

1. D. J. Hucknall, "Selective oxidation of Hydrocarbons." Academic Press, London/New York, 1977.
2. A. Andersson and S. Hansen, *Catal. Lett.* **1,** 377 (1988).
3. A. Andersson and S. Hansen, *J. Catal.* **114,** 332 (1988).
4. B. C. Gates, J. R. Katzer, and G. C. A. Schuit, "Chemistry of Catalytic Processes," p. 390. McGraw–Hill, New York, 1979.
5. J. von Destinon-Forstmann, *Can. Metall. Q.* **4,** 1 (1965).
6. Ph. A. Batist, C. J. Kapteijns, B. C. Lippens, and G. C. A. Schuit, *J. Catal.* **7,** 33 (1967).
7. D. M. Tschishikov, Yu. E. Ratner, and Yu. V. Tsvetkov, *Izv. Akad. Nauk SSSR Met.* No. 6, 8 (1970).
8. F. E. Massoth, *J. Catal.* **30,** 204 (1973).
9. M. J. Kennedy and S. C. Bevan, *J. Less-Common Met.* **36,** 23 (1974).
10. P. Ratnasamy, A. V. Ramaswamy, K. Banerjee, D. K. Sharma, and N. Ray, *J. Catal.* **38,** 19 (1975).
11. R. Burch, *J. Chem. Soc. Faraday Trans. 1* **74,** 2982 (1978).
12. J. Orehotsky, L. Jamiolkowski, and J. Gerboc, *Mater. Sci. Eng.* **41,** 237 (1979).
13. P. Gajardo, P. Grange, and B. Delmon, *J. Phys. Chem.* **83,** 1771 (1979).
14. A. Ueno and C. O. Bennett, *Bull. Chem. Soc. Jpn.* **52,** 2551 (1979).
15. A. Ueno, Y. Kotera, S. Okuda, and C. O. Bennett, "Chemistry and Uses of Molybdenum," Proceedings, 5th International Conference, p. 250. Climax Molybdenum Co., Ann Arbor, MI, 1982.
16. J. Słoczyński, *React. Solids* **7,** 83 (1989).
17. J. Słoczyński and W. Bobiński, *J. Solid State Chem.* **92,** 420 (1991).
18. J. Słoczyński and W. Bobiński, *J. Solid State Chem.* **92,** 436 (1991).
19. P. Barret, "Cinetique Heterogene." Gauthier-Villars, Paris, 1973.
20. O. Glemser and G. Lutz, *Z. Anorg. Allg. Chem.* **264,** 17 (1951).
21. O. Glemser, G. Lutz, and G. Meyer, *Z. Anorg. Allg. Chem.* **285,** 173 (1956).
22. A. Magneli, G. Andersson, B. Blomberg, and L. Kihlborg, *Anal. Chem.* **24,** 1998 (1952).
23. L. Kihlborg, *Acta Chem. Scand.* **13,** 954 (1959).
24. A. Sárdi, *Acta Chim. Hung.* **39,** 145 (1963).
25. D. T. Hawkins and W. L. Worrell, *Metall. Trans.* **1,** 271 (1970).
26. Yu. M. Solonin, *Poroshk. Metall.* No. 4, 1 (1979).
27. S. Hansen and A. Andersson, *J. Solid State Chem.* **75,** 225 (1988).
28. L. A. Bursill, *Proc. R. Soc. London A* **311,** 267 (1969).
29. W. Thöni and P. B. Hirsch, *Philos. Mag.* **33,** 639 (1976).
30. W. Thöni, P. L. Gai, and P. B. Hirsch, *J. Less-Common Met.* **54,** 263 (1977).
31. P. L. Gai and M. J. Goringe, *Krist. Tech.* **14,** 1385 (1979).
32. P. L. Gai, *Philos. Mag.* **43,** 841 (1981).
33. E. L. Aptekar, M. G. Chudinov, A. M. Alekseev, and O. V. Krylov, *React. Kinet. Catal. Lett.* **1,** 493 (1974).
34. A. Cimino and B. A. De Angelis, *J. Catal.* **36,** 11 (1975).
35. J. Haber, W. Marczewski, J. Stoch, and L. Ungier, *Ber. Bunsenges. Phys. Chem.* **79,** 970 (1975).
36. K. S. Seshadri and L. Petrakis, *J. Catal.* **30,** 195 (1973).
37. N. Giordano, A. Castellan, J. C. J. Bart, A. Vaghi, and F. Campadelli, *J. Catal.* **37,** 204 (1975).
38. E. Serwicka, *J. Solid State Chem.* **51,** 300 (1984).
39. P. A. Sermon and G. C. Bond, *J. Chem. Soc. Faraday Trans. 1* **72,** 730 (1976).
40. T. H. Fleisch and G. J. Mains, *J. Chem. Phys.* **76,** 780 (1982).
41. R. Erre, H. Van Damme, and J. J. Fripiat, *Surf. Sci.* **127,** 48 (1983).
42. X. Lin, J. F. Lambert, J. J. Fripiat, and C. Ancion, *J. Catal.* **119,** 215 (1989).
43. N. I. Iltschenko, V. A. Yuza, and V. A. Roiter, *Dokl. Akad. Nauk SSSR* **172,** 133 (1967).
44. K. M. Sancier, *J. Catal.* **23,** 298 (1971).
45. N. I. Iltschenko, *Usp. Khim.* **41,** 84 (1972).
46. I. V. Uvarova, V. V. Panitschkina, and L. D. Kontschakovskaya, *Izv. Akad. Nauk SSSR Met.* No. 4, 86 (1972).
47. I. V. Uvarova, *Izv. Akad. Nauk SSSR, Met.* No. 4, 38 (1974).
48. T. Fransen, P. C. Van Berge, and P. Mars, *React. Kinet Catal. Lett.* **5,** 445 (1976).

49. O. Levenspiel, "Chemical Reaction Engineering," p. 357. Wiley, New York, 1972.
50. L. V. Gurvitch, G. V. Karatchevsev, V. N. Kondratev, Yu. A. Lebedev, V. A. Medvedev, V. K. Potapov, and Yu. S. Khodeev, "Dissociation Energies. Ionization Potentials and Electron Affinities." Nauka, Moscow, 1974. (in Russian)
51. J. C. Volta, M. Forissier, F. Theobald, and T. P. Pham, *Faraday Discuss. Chem. Soc.* **72,** 225 (1981).
52. J. C. Volta, J. M. Tatibouet, C. Prichitkul, and J. E. Germain, *in* "Proceedings, 8th International Congress of Catalysis, Berlin, 1984," Vol. IV, p. 451. Dechema, Frankfurt-am-Main, 1984.
53. J. C. Volta and J. M. Tatibouet, *J. Catal.* **93,** 467 (1985).
54. J. Ziółkowski, *J. Catal.* **80,** 263 (1983).
55. K. Brückman, R. Grabowski, J. Haber, A. Mazurkiewicz, J. Słoczyński, and T. Wiltowski, *J. Catal.* **104,** 71 (1987).
56. J. M. Tatibouet and J. E. Germain, *J. Chem. Res.* **5,** 268 (1981).
57. J. M. Tatibouet, J. E. Germain, and J. C. Volta, *J. Catal.* **82,** 240 (1983).
58. J. M. Dominguez-Esquivel, O. Guzmán-Mandujano, and A. Garcia-Bórquez, *J. Catal.* **103,** 200 (1987).
59. B. Mingot, N. Floquet, O. Bertrand, M. Treilleux, J. J. Heizmann, J. Massardier, and M. Abon, *J. Catal.* **118,** 424 (1989).
60. M. Abon, J. Massardier, B. Mingot, J. C. Volta, N. Floquet, and O. Bertrand, *J. Catal.* **134,** 542 (1992).
61. J. G. Steenhof De Jong, C. H. E. Guffens, and H. S. Van Der Baan, *J. Catal.* **31,** 149 (1973).